




# Expression of the ectodomain-releasing protease ADAM17 is directly regulated by the osteosarcoma and bone-related transcription factor RUNX2

Héctor F. Araya<sup>1,2</sup> | Hugo Sepulveda<sup>3</sup>  | Carlos O. Lizama<sup>4</sup> |  
Oscar A. Vega<sup>1,2</sup> | Sofia Jerez<sup>1,2</sup> | Pedro F. Briceño<sup>1,2</sup> | Roman Thaler<sup>5,6</sup> |  
Scott M. Riester<sup>5,6</sup> | Marcelo Antonelli<sup>1</sup> | Flavio Salazar-Onfray<sup>2,7</sup> |  
Juan Pablo Rodríguez<sup>8</sup> | Ricardo D. Moreno<sup>4</sup> | Martin Montecino<sup>3</sup> |  
Martine Charbonneau<sup>9</sup> | Claire M. Dubois<sup>9</sup> | Gary S. Stein<sup>10</sup> |  
Andre J. van Wijnen<sup>5,6</sup>  | Mario A. Galindo<sup>1,2</sup> 

<sup>1</sup> Program of Cellular and Molecular Biology, Institute of Biomedical Sciences, Faculty of Medicine, University of Chile, Santiago, Chile

<sup>2</sup> Millennium Institute on Immunology and Immunotherapy, Faculty of Medicine, University of Chile, Santiago, Chile

<sup>3</sup> Center for Biomedical Research, Faculty of Biological Sciences and Faculty of Medicine, FONDAF Center for Genome Regulation, Universidad Andres Bello, Santiago, Chile

<sup>4</sup> Departamento de Fisiología, Facultad de Ciencias Biológicas, Pontificia Universidad Católica de Chile, Santiago, Chile

<sup>5</sup> Department of Orthopedic Surgery, Mayo Clinic, Rochester, Minnesota

<sup>6</sup> Department of Biochemistry and Molecular Biology, Mayo Clinic, Rochester, Minnesota

<sup>7</sup> Program of Immunology, Institute of Biomedical Sciences, Faculty of Medicine, University of Chile, Santiago, Chile

<sup>8</sup> Instituto de Nutrición y Tecnología de los Alimentos (INTA), University of Chile, Santiago, Chile

<sup>9</sup> Immunology Division, Department of Pediatrics, Faculty of Medicine and Health Sciences, University of Sherbrooke, Sherbrooke, Quebec, Canada

<sup>10</sup> Department of Biochemistry and University of Vermont Cancer Center, The Robert Larner MD College of Medicine, University of Vermont, Burlington, Vermont

## Correspondence

Mario A. Galindo, Institute of Biomedical Sciences, Faculty of Medicine, University of Chile, Av. Independencia 1027, ZIP code 8380453, Santiago, Chile.  
Email: mgalindo@med.uchile.cl

## Funding information

National Institutes of Health, Grant numbers: R01 AR049069, P01 CA082834; Scientific and Technological Development Support Fund (FONDEF, Chile), Grant number: ID16110148; Millennium Science Initiative From Ministry for Economy, Development and Tourism, Chile, Grant number: P09/016F; National Fund for Scientific and

## Abstract

Osteoblast differentiation is controlled by transcription factor RUNX2 which temporally activates or represses several bone-related genes, including those encoding extracellular matrix proteins or factors that control cell-cell, and cell-matrix interactions. Cell-cell communication in the many skeletal pericellular micro-niches is critical for bone development and involves paracrine secretion of growth factors and morphogens. This paracrine signaling is in part regulated by “A Disintegrin And Metalloproteinase” (ADAM) proteins. These cell membrane-associated metalloproteinases support proteolytic release (“shedding”) of protein ectodomains residing at the cell surface. We analyzed microarray and RNA-sequencing data for *Adam* genes and show that *Adam17*, *Adam10*, and *Adam9* are stimulated during BMP2 mediated induction of osteogenic differentiation and are

Present address of Carlos O. Lizama is Cardiovascular Research Institute, University of California, San Francisco, CA 94143, USA.

Present address of Oscar A. Vega is Hospital Regional de Coyhaique, Servicio de Urgencia, XI Región de Aysén, Chile.

Technological Development (FONDECYT, Chile), Grant numbers: 1095234, 1130931, 1130706, 1171213, 1160214, 1110778, 1150352; Fund for Research Centers in Priority Areas (FONDAP, Chile), Grant number: 15090007

robustly expressed in human osteoblastic cells. ADAM17, which was initially identified as a tumor necrosis factor alpha (TNF $\alpha$ ) converting enzyme also called (TACE), regulates TNF $\alpha$ -signaling pathway, which inhibits osteoblast differentiation. We demonstrate that *Adam17* expression is suppressed by RUNX2 during osteoblast differentiation through the proximal *Adam17* promoter region (−0.4 kb) containing two functional RUNX2 binding motifs. *Adam17* downregulation during osteoblast differentiation is paralleled by increased RUNX2 expression, cytoplasmic-nuclear translocation and enhanced binding to the *Adam17* proximal promoter. Forced expression of *Adam17* reduces *Runx2* and *Alpl* expression, indicating that *Adam17* may negatively modulate osteoblast differentiation. These findings suggest a novel regulatory mechanism involving a reciprocal *Runx2-Adam17* negative feedback loop to regulate progression through osteoblast differentiation. Our results suggest that RUNX2 may control paracrine signaling through regulation of ectodomain shedding at the cell surface of osteoblasts by directly suppressing *Adam17* expression.

#### KEYWORDS

ADAM genes, ADAM17, osteoblast differentiation, RUNX2, transcriptional regulation

## 1 | INTRODUCTION

Differentiation of osteoblast lineage cells requires the complex genetic and biochemical interplay of gene regulatory signaling pathways, including BMPs, WNTs, FGFs, PTH, IGF, GPNMB/osteostatin, CTGF/CCN2, and several key transcription factors (eg RUNX2, OSX/SP7, DLX5, ATF4, SATB2).<sup>1–10</sup> The essential role of RUNX2 during osteoblast maturation is reflected by severe bone phenotypes resulting from genetic mutations that abrogate the normal functions of RUNX2, its partner C/EBP $\beta$ , or its downstream target Osterix/SP7 in mouse models, and human disease.<sup>1,2,11–16</sup> Consistent with the central role of RUNX2 in skeletal development and bone formation, the expression of the *Runx2* gene is tightly controlled by chromatin-dependent mechanisms, multiple protein/DNA interactions and three-dimensional chromatin loops.<sup>17–22</sup> In addition, *Runx2* expression is post-transcriptionally controlled by multiple miRNAs that regulate osteoblast differentiation<sup>23–27</sup> and the mitotic partitioning of *Runx2* mRNA in proliferating osteoblasts.<sup>28</sup> The broad biological functions of RUNX2 in osteoblasts are reflected by its intrinsic ability to activate a large cohort of target genes in a cell-stage specific manner.<sup>29–38</sup>

The ADAM (A Disintegrin and Metalloproteinase) proteins are a family of transmembrane metalloproteinases containing an extracellular catalytic domain implicated in ectodomain shedding of different cell surface proteins (ie growth factors, cytokines, receptors, and cell adhesion molecules). The ADAM proteins are closely related to

ADAMTS (A Disintegrin And Metalloproteinase with Thrombospondin motifs), a group of secreted metalloproteinases that mediate proteolytic processing or degradation of specific extracellular matrix (ECM) molecules (eg procollagen and aggrecan). ADAM proteins may affect the bone micro-niche through juxtacrine and paracrine effects by cleaving extracellular regions of cell surface associated proteins (ectodomain shedding). For example, these proteins have potent effects on multiple regulatory pathways including those involving fibroblast growth factor receptor 2 (FGFR2), insulin-like growth factor binding protein 5 (IGFBP5), interleukin-6 receptor (IL6R), and Notch receptors in osteoblasts.<sup>39–45</sup> Other roles that ADAMs perform in the bone micro-environment include effects on Notch modulators, receptor activator of NF-kappaB ligand (RANKL), as well as other mechanisms in osteoclasts, chondrocytes, and bone-metastatic tumor cells.<sup>46–49</sup> To gain insight into the biological roles of ADAM proteins in osteoblastogenesis and bone formation, it is necessary to assess which *Adam* genes are expressed in bone cells.

Previous studies have shown that ADAM (ADAM8, 9, 10, 12, 15, 17, and 19) and ADAMTS (ADAMTS1, 4, and 5) family members are expressed in osteoblastic cells and bone tissue<sup>41,50–56</sup> and has been demonstrated that some of them shown significant changes in its expression levels during osteoblast differentiation.<sup>39,57</sup> Moreover, *Adamts4* and *Adamts5* genes have been reported to be direct downstream targets of RUNX2 in chondrocytes.<sup>58–62</sup> Collectively, these data suggest that *Adam* and *Adamts* genes are differentially

expressed during osteoblast differentiation and that RUNX2 may transcriptionally control the expression of members of the ADAM and ADAMTS families. Particularly, conditional inactivation of *Adam17* gene in osteochondroprogenitor cells results in several defects including increased osteoblast numbers, suggesting potential functions related to bone formation.<sup>63</sup> ADAM17, also known as TNF- $\alpha$  converting enzyme (TACE), is a membrane-anchored metalloproteinase that cleaves diverse cell surface proteins (ie cytokines, cell adhesion proteins, and cell growth factor receptors) including, interestingly, the type II membrane-bound precursor of TNF $\alpha$ , a known inhibitor of osteoblast differentiation.<sup>64</sup> Because of pleiotropic defects observed in *Adam17* conditional knockout mice, we dissected molecular mechanisms controlling *Adam17* functions using cell culture models.

In this study, we show that osteoblastic cell types express multiple members of the ADAM family and the relatively abundantly expressed members ADAM9, ADAM10, and ADAM17 exhibit significant changes in gene expression levels during osteogenic differentiation. We show that RUNX2 directly attenuates *Adam17* gene expression via selective recruitment of RUNX2 through a functional binding site contained in the proximal promoter of the *Adam17* gene and that the C-terminal transactivation region of RUNX2 is essential for repression of the *Adam17* promoter. Our study suggests that RUNX2 may control ectodomain shedding in the pericellular micro-environment of osteoblasts to control the cell-cell communication through the regulation of *Adam17* gene expression.

## 2 | MATERIALS AND METHODS

### 2.1 | Cell culture

Mouse MC3T3-E1 osteoblasts, mouse pre-myogenic mesenchymal C2C12 precursor cells, rat osteosarcoma ROS17/2.8 cells, and human osteosarcoma cell lines (SAOS-2, MG63, U2OS, G292, HOS, and 143B cells) were obtained from the American Type Culture Collection (ATCC, Manassas, VA). Immortalized mouse *Runx2* null (*Runx2*<sup>-/-</sup>) calvarial osteoprogenitor cells were described previously.<sup>65</sup> Cells were maintained in culture medium supplemented with 5–15% fetal bovine serum (FBS) (HyClone Laboratories Inc, Logan, UT) plus 2 mM L-glutamine and a penicillin-streptomycin cocktail at 37°C and 5% CO<sub>2</sub> humidified atmosphere. MC3T3-E1 and *Runx2*<sup>-/-</sup> cells were cultured in  $\alpha$ MEM medium (Gibco, Grand Island, NY) supplemented with 10% FBS. C2C12 cells were cultured in DMEM medium (Gibco) supplemented with 10% FBS. ROS17/2.8 cell were grown in F12 medium (Gibco) supplemented with 5% FBS. SAOS cells were maintained in McCoy's medium (Sigma-Aldrich, St Louis, MO) supplemented with 15% FBS. U2OS and G292 cells were cultured in McCoy's medium with 10%

FBS. MG63 and HOS cells were grown in DMEM medium with 10% FBS. 143B cells were maintained in DMEM medium, 1 mM sodium pyruvate, 100  $\mu$ g/mL of bromodeoxyuridine and 10% FBS. The growth medium was changed every 2 days. Primary osteoblastic outgrowth cultures for RNA-seq analysis were obtained from distal femur or proximal tibia bone specimens obtained as surgical waste samples with approval of the Mayo Clinic Institutional Review Board. Samples were manually minced and crushed with a scalpel and cells were allowed to grow for one passage until confluence in standard media using procedures described previously.<sup>66</sup>

### 2.2 | Osteoblast differentiation

For in vitro differentiation studies, MC3T3-E1 cells were plated in 100-mm or 60-mm plates or in 6-well plates and grown in regular medium up to confluence. Confluent cells were treated with 0.1  $\mu$ M dexamethasone, 10 mM  $\beta$ -glycerophosphate, and 50  $\mu$ g/mL ascorbic acid in fresh regular media and cultured for 22 days. Media was changed every two days for the remainder of the experiment and cells were harvested at selected time points (at days 0, 4, 8, 12, 16, and 22 of their osteogenic differentiation) for Western blot, RT-PCR and immunohistochemistry. Cell cycle exit was determined by monitoring cyclin D1 (CCND1) expression. The capacity of cells to differentiate into the osteoblastic lineage was evaluated by monitoring *Runx2* and alkaline phosphatase (*Alpl*) mRNA levels, as well as RUNX2 levels and ALPL activity.

### 2.3 | DNA transfection and adenoviral infection

Subconfluent *Runx2*<sup>-/-</sup> cells or MC3T3-E1 cells were transiently transfected with pcDNA-*Runx2*, deletion mutant *Runx2* 1-361 (*Runx2*  $\Delta$ C), pcDNA-*Adam17*, or pcDNA-empty vector (control) using Lipofectamin 2000® reagent (Invitrogen, Carlsbad, CA) according to the manufacturer's recommendations. Adenoviral delivery of vector containing the cDNA of *Runx2* coupled to Green Fluorescent Protein (GFP) (*Runx2*-IRES-*gfp*) under control of the CMV5 promoter was used as previously described.<sup>67</sup> Preparation and purification of virus were performed according to the manufacturer's protocols (Promega, Madison, WI). For control of infection, the same Adenovirus vector carrying *gfp* was used. The Adenovirus *Runx2* (Adv-*Runx2*) contains both the *gfp* cassette and the *Runx2* cDNA in forward orientation (+) and Adenovirus Vector (Adv-Vector) contains the *gfp* cassette in the forward orientation (+) and the *Runx2* cDNA in reverse orientation (-).<sup>67</sup> *Runx2*<sup>-/-</sup> cells were plated for infections in 60 mm plates at a density of  $3 \times 10^5$  cells/plate and cultured in DMEM with 10% FBS.

After 24 h, cells were infected at 60–70% of confluence with  $30 \times 10^{10}$  OPU/mL (optical particle unit) of each virus in 900  $\mu$ L of DMEM supplemented with 1% FBS for 4 h. Upon addition of 600  $\mu$ L of media containing 1% FBS, cells were incubated for an additional 10 h. After adenoviral infection, cells were grown for 24–72 h. Infection efficiencies were assessed by activity of GFP using a Nikon Diaphot inverted fluorescence microscope.

## 2.4 | Western blot analysis

RUNX2, ADAM17, CCND1, and  $\beta$ -actin/ACTB were analyzed by Western blot analysis as described previously.<sup>68,69</sup> Briefly, equal amounts of total cellular protein collected in the presence of the proteasome inhibitor MG132 (Calbiochem, San Diego, CA) and Complete cocktail of protease inhibitor (Roche Diagnostics, Mannheim, Germany) were resolved in 10% SDS-PAGE and transferred to polyvinylidene difluoride membranes (Perkin Elmer, Boston, MA). Blots were incubated with a 1:2,000 dilution of each primary antibody for 1 h. RUNX2-specific mouse monoclonal antibody 8G5 (MBL International, Woburn, MA), ADAM17 rabbit polyclonal antibody (Anti-TACE 807-823) (Calbiochem), CCND1 mouse monoclonal antibody DCS-6 (sc-20044) (Santa Cruz Biotechnology Inc., Santa Cruz, CA) and  $\beta$ -actin goat polyclonal antibody C-11 (sc-1615) (Santa Cruz Biotechnology) were acquired commercially. Membranes were incubated with the respective horseradish peroxidase-conjugated secondary antibody (sc-2005 anti-mouse or sc-2004 anti-rabbit or sc-2020 anti-goat) (Santa Cruz Biotechnology) for 1 h. Immuno-reactive protein bands were visualized on a Kodak BioMax Light film (Carestream Health Inc, Rochester, NY) using a chemiluminescence detection kit (Thermo Fisher Scientific, Rockford, IL). Signal intensities were quantified by densitometry.

## 2.5 | RNA-sequencing (RNA-seq) and semi-quantitative PCR

RNA-sequencing analysis of select samples from human osteosarcoma cells and osteoblastic bone-derived cells was performed using Illumina 2000 instrumentation and subsequently analyzed using a standardized bioinformatics pipeline (Bioinformatics Core at Mayo Clinic) as described in detail previously.<sup>70</sup> Expression values are denoted as reads per kilobase per million mapped reads (RPKM). Expression of select genes was visualized and validated by semi-quantitative PCR. Total RNA was isolated using TRIzol reagent (Invitrogen) according to the manufacturer's specifications. Total RNA (5  $\mu$ g/lane) was separated in a 1% agarose-formaldehyde gel. Ethidium bromide staining of the gels was used to assess RNA quality of samples. Purified RNA (3  $\mu$ g) was treated with RQ1RNase-Free DNase (Promega) and

subjected to reverse transcription using random hexamer primers (Promega) with M-MLV reverse transcriptase (Promega) according to the manufacturer's recommendations. Gene expression was assessed by PCR using the following specific mouse (m) and human (h) gene primers (0.5 pmol/ $\mu$ L): m/r/h*Runx2*: F 5'-CCGCACGACAACCGCACCAT-3', R 5'-CGCTCCGGCCACAAATCTC-3'; m/h*Adam9*: F 5'-CAGACTGCTGTGAGAGAAG-3', R 5'-CATTCTGCAGTTCCACCA-3'; m/h*Adam10*: F 5'-CCTACGAATGAAGAGGGAC-3', R 5'-ATCACAGCTTCTCGTGTTC-3'; m/r/h*Adam17*: F 5'-GACATGAATGGCAAATGTGA-3', R 5'-TGGACAAGAATGCTGAAAGGA-3'; m*Alpl*: F 5'-TCCATCCTGCGCTGGGCCAA-3', R 5'-GGCCAGCAGTTCAGTGCGGT-3'; m/r/h*Gadph*: F 5'-CCTTCATTGACCTCAACTA-3', R 5'-GGCCATCCACAGTCTTCT-3'. PCR amplification of cDNAs was carried out using 1 $\times$  PCR buffer (Promega) containing 0.2 mM dNTPs (Promega), 1.5 mM MgCL (Promega), 0.06 U/ $\mu$ L of Taq polymerase (Invitrogen) by incubation for 5 min at 94°C and 20–30 amplification cycles of synthesis were applied to avoid product saturation (1 min at 94°C, 1 min at 52–62°C, and 1 min at 72°C), followed by a final extension step at 72°C for 6 min. Aliquots of the resulting products (5  $\mu$ L) were visualized in 1% agarose gels by ethidium bromide staining.

## 2.6 | Alkaline phosphatase (AP) activity

Differentiating MC3T3-E1 cells in 6-well plate or 60 mm plate were washed with PBS and then fixed with 4% paraformaldehyde for 30 s. AP activity was detected by colorimetric reaction using the AP liquid substrate nitro blue tetrazolium and 5-bromo-4-chloro-3-idolyl phosphate (NBT/BCIP) (Roche Diagnostics, Mannheim, Germany). AP staining solution (NTB 0.4 mg/mL and BCIP 0.19 mg/mL in 100 mM Tris buffer, 50 mM MgSO<sub>4</sub>, pH 9.5) was added to each well and staining was carried out at 37°C for 25 min. NBT/BCIP colorimetric reactions were stopped by aspirating the staining solution and rinsing the cells twice in PBS. AP positive cells were detected and photographed under a Zeiss Axiostar Plus light microscope.

## 2.7 | Immunohistochemistry

MC3T3-E1 cells were washed twice with PBS and collected in a 1.5 mL tube using a scraper followed by centrifugation at 380g for 2 min. The cell pellets were fixed with formalin for 24 h, dehydrated and embedded in paraffin using standard procedures. Paraffin-embedded cells were sectioned (5  $\mu$ m), adhered to glass slides, and rehydrated, and antigens were recovered by treatment with retrieval buffer (1 mM Tris, 0.5 mM EGTA, pH 9.0). Sections were blocked with PBS supplemented with 1% bovine serum albumin. Then sections were incubated with 1:100 dilution of RUNX2 rabbit

polyclonal antibody M-70 (sc-10758) (Santa Cruz Biotechnology) or ADAM17 rabbit polyclonal antibody, washed and then incubated with 1:200 dilution of the indicated biotinylated secondary antibody. Finally, antibodies bind to specific antigens were detected using a biotin-streptavidin detection system. Samples were observed under a Zeiss Axiostar Plus light microscope.

## 2.8 | Luciferase reporter assays

For reporter assays, MC3T3-E1 cells were seeded at  $8 \times 10^4$  cells/well in a 6-well plate and transiently transfected 24–48 h after plating at a cell density of 60–70% with 1  $\mu$ g of the previously described construct *Tace* promoter/pGL2 luciferase reporter plasmid which contains the 2.304-kb mouse proximal *Tace* promoter fused to the *firefly* luciferase reporter.<sup>71</sup> Alternatively, cells were transiently transfected with a series of *Tace* promoter 5' deletants: p*Tace*-1567, –903, –410, and –121, which were generated by digestion of the p*Tace*-Luc vector with the appropriate restriction enzymes.<sup>71</sup> Cells were co-transfected with 10 ng SV40/*Renilla* luciferase plasmid (pRL-SV40) as an internal control. The promoterless pGL2 luciferase parent vector was used as a negative control. Lipofectamine 2000 was used as a transfection agent according to the manufacturer's protocol and transfections were performed in absence of FBS and antibiotics. Medium was changed after 4 h to normal growth medium with FBS and antibiotics. Twenty-four hours after transfection, cells were harvested in 1 $\times$  passive lysis buffer and luciferase activity was measured in cell lysates using the Dual Luciferase Reporter Assay System® kit (Promega) following the manufacturer's instructions. Luminescent signal was quantified by a luminometer (Synergy® 2SL BioTek), and each measurement from the *firefly* luciferase construct was normalized using *Renilla* luciferase values.

## 2.9 | Chromatin immunoprecipitation (ChIP) analysis

ChIP assays studies were performed as described previously.<sup>72</sup> Pre-cleared chromatin fragments (200 to 300 bp) obtained from MC3T3-E1 cells were immunoprecipitated overnight with agitation using anti-RUNX2 M70 polyclonal antibodies. The PCR primers used to evaluate the proximal (–400/–167), middle (–930/–731), and distal (–1651/–1422) regions of the mouse *Adam17* promoter by Quantitative real-time PCR were: (–400/–167): F 5'-GGACAGAGGCGAGAGAGAGA-3', R 5'-GCTGAGAGCGGCTTAACTC-3'; (–930/–731): F 5'-GCAAGACATTCCACAACGAA-3', R 5'-AGTGAACAGGAGCGCACATC-3'; (–1651/–1422): F 5'-AGTGGCACTCAGCCTTCCTA-3', R 5'-GTACTCAACCCCTTGGGTCA-3'. Q-PCR was performed using the Brilliant II SYBR Green

Q-PCR Master Mix (Agilent Technologies, Santa Clara, CA) in an Mx3000P spectrofluorometric thermal cycler (Stratagene-Agilent, Santa Clara, CA) according to the manufacturer's recommendations.

## 2.10 | Statistical analysis

Data were represented as mean  $\pm$  SEM with a minimum of three independent samples and analyzed using Student's *t*-test. *P* value of less than 0.05 was considered statistically significant.

# 3 | RESULTS

## 3.1 | Identification of BMP-2-responsive and abundantly expressed ADAM genes in the osteogenic cell lineage

To identify Adam genes that would be involved in the osteoblast differentiation process, we determined gene expression patterns of these genes at early stages of osteogenic lineage commitment in C2C12 mesenchymal progenitor cells stimulated with the Bone Morphogenetic Protein 2 (BMP-2). This cell culture model system focuses on the first stages of osteogenic lineage-commitment (1–24 h) in response to BMP2/BMPR/SMAD signaling and the initial activation of osteoblast specific gene expression programs as evidenced by microarray gene expression profiling.<sup>73</sup> Examination of these published data revealed that three *Adam* genes are upregulated (*Adam17*, *Adam10*, and *Adam9*) between 4 and 12 h after BMP-2 treatment (Figure 1A) and three genes are downregulated (*Adam8*, *Adam15*, and *Adam19*) (Figure 1B). Expression analysis of ADAM genes by RNA-seq reveals that the same group of BMP-2 responsive genes are the most abundantly expressed ADAM genes in primary human osteoblastic bone derived cells (hOBs) and collectively cover the ~97% of all ADAM transcripts in this cells (Figure 1C). Further expression analysis of the three BMP2- upregulated ADAMs in other cell types revealed that expression of *ADAM17*, *ADAM10*, and *ADAM9* is rather constant in human primary osteoblastic bone-derived cells (ie hOB1, hOB2, and hOB3), but its expression appears to be more variable in osteosarcoma cell types (Figure 1D–F). Hence, cells in the osteogenic lineage express a limited number of ADAMs genes, and their expression may be selectively modulated in osteosarcoma cell types.

## 3.2 | RUNX2 modulates Adam17 gene expression

Because conditional in vivo inactivation of *Adam17* gene exhibited several bone-related defects including increased osteoblast numbers and because ADAM17 protein is an

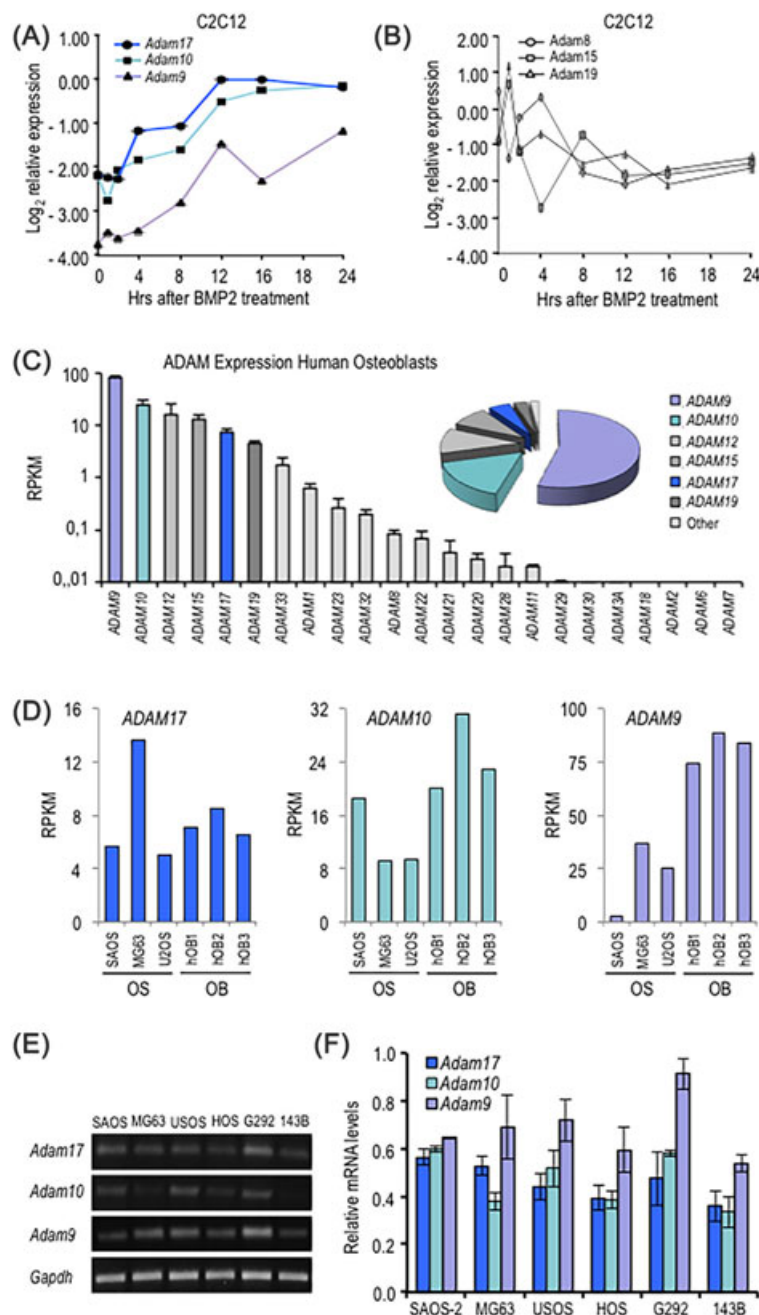


**FIGURE 1** *Adam17*, *Adam10*, and *Adam9* gene expression is up regulated during early stage of commitment and differentiation to the osteoblast phenotype and stably expressed in human immature osteoblastic cells. To identify genes that immediately respond to osteogenic stimuli, we retrieved microarray data were retrieved for experiments with mouse C2C12 mesenchymal cells that were treated with 300 ng/mL of BMP-2 and analyzed at distinct time points (0, 4, 8, 12, 16, 20, and 24 h). Data on ADAM genes were filtered for genes that show more than a twofold change in gene expression. This analysis revealed that the *Adam17*, *Adam10*, and *Adam9* genes are upregulated for more than twofold (A), while three others are downregulated (*Adam8*, *Adam15*, *Adam19*) (B). C, The bar graph shows average expression values (in RPKM; STD as error bar for  $n = 3$  human donors) that were rank ordered for relative expression based on RNA-seq analysis of human osteoblastic bone-derived cells from three different donors. The pie chart presented in the inset shows that the six most highly expressed ADAM genes (including the BMP-responsive ADAMs *ADAM17*, *ADAM10*, and *ADAM9*, which are presented in color) account for almost all (~97%) ADAM-related transcripts. D, Results of RNA-seq analysis for each individual donor and select osteosarcoma cell lines (SaOS-2, MG63, and U2OS) as indicated. E, Visual presentation and validation of gene expression data using semi-quantitative RT-PCR and ethidium bromide staining. *ADAM17*, *ADAM10*, and *ADAM9* gene expression was assessed as indicated in human SAOS-2, MG63, U2OS, HOS, G292, and 143B immature osteoblast cells. The data shown are representative of three experiments with similar outcomes. The graphs show quantification of the RT-PCR data relative to *Gapdh* mRNA (F). All data are presented as mean  $\pm$  SEM from three independent experiments

important regulator of TNF $\alpha$ -signaling pathway that inhibits osteoblast differentiation, we focused our subsequent analyses on the molecular mechanism that control the expression of *Adam17* during osteoblast differentiation.

We first investigated whether there is a functional coupling between RUNX2 and *Adam17* expression in *Runx2*-null calvarial cells compared to several osteoblastic cell lines. In agreement with our bioinformatics analyses, both *Runx2* and *Adam17* are expressed at detectable mRNA and

protein levels in osteoblastic cell types (MC3T3-E1, ROS17/2.8, and SAOS-2 cells). Interestingly, depletion of RUNX2 expression in *Runx2* null cells results in significant increases of *Adam17* expression (Figure 2A-D). This finding suggests that *Adam17* expression is negatively regulated by RUNX2. This possibility is supported by a robust decrease in *Adam17* expression induced by overexpression of *Runx2* in the same *Runx2*-null cells (Figure 2E-H). Importantly, dosing experiments using different amounts of expression vector reveal that

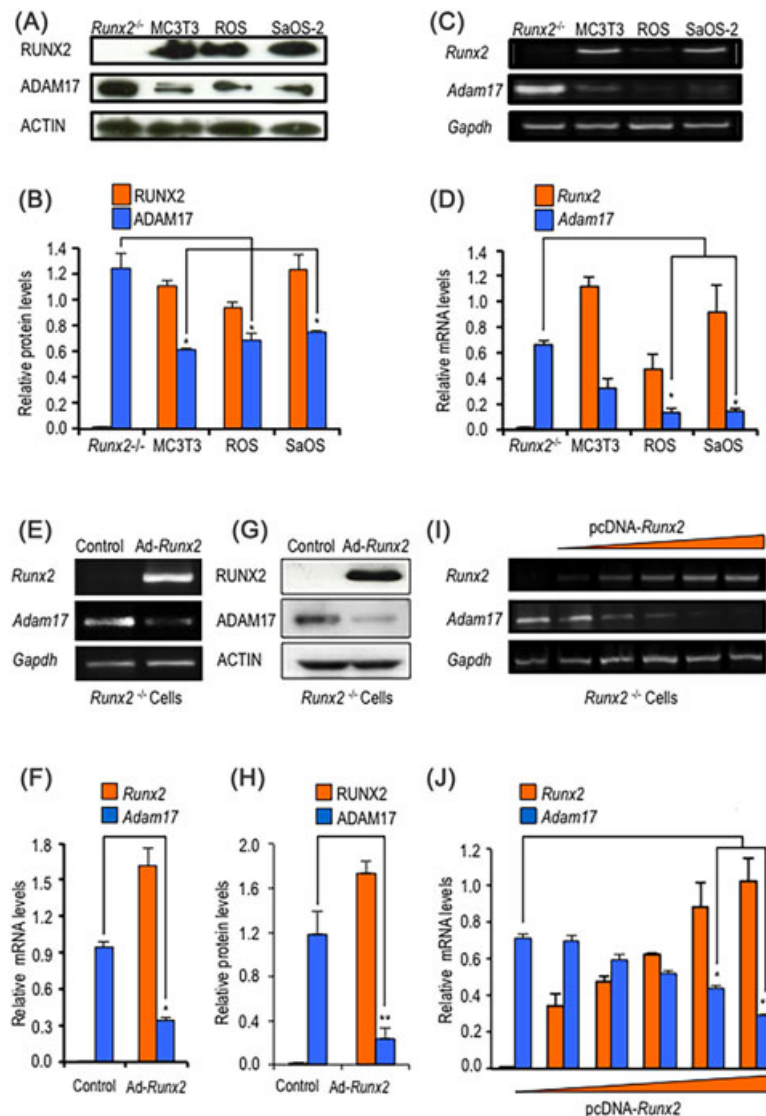


**FIGURE 2** *Adam17* gene expression is negatively regulated by RUNX2. *Adam17* and *Runx2* expression was assessed in mouse *Runx2*-null osteoprogenitor cells (*Runx2*<sup>-/-</sup>) and mouse MC3T3-E1 pre-osteoblasts cells, as well as rat ROS17/2.8 and human SAOS-2 osteosarcoma cells. Protein and mRNA levels were evaluated by western blot analysis (A, and down graph B) and RT-PCR (C, and down graph D), respectively. *Runx2*-null cells were infected with an adenovirus vector expressing RUNX2 or GFP (control) as indicated (E and G). Alternatively, cells were transiently transfected with different concentrations (0.5, 1, 2.5, 5, and 10  $\mu$ g of DNA) of pcDNA-*Runx2* or pcDNA-empty vector (control) (I). *Runx2*-null cells expressing *Adam17* and *Runx2* mRNA (E, I, and down graph F and J) and protein levels (G, and down graph H) were evaluated by RT-PCR and Western blot analysis, respectively. The data shown are representative of three experiments with similar outcomes. *Adam17* and *Runx2* mRNA and protein values were normalized to *Gapdh* and Actin, respectively. All data are presented as mean  $\pm$  SEM from three independent experiments. \* $P < 0.05$  and \*\* $P < 0.01$

*Adam17* expression is inversely proportional to the amount of exogenous *Runx2* expressed in *Runx2* null cells (Figures 2I and 2J). Hence, our data indicate that RUNX2 suppresses *Adam17* mRNA and protein expression levels in osteogenic lineage cells.

### 3.3 | *Adam17* gene is directly regulated by RUNX2 at the promoter level in committed osteoblasts

Considering the inverse correlation between the expression levels of *Runx2* and *Adam17*, we hypothesized that *Adam17* can be a direct transcriptional target of RUNX2 during osteoblast differentiation. In silico analysis of the mouse, rat and human *Adam17* promoter sequences identified several potential RUNX2 binding sites. The mouse promoter exhibits nine transcription start site (TSS)<sup>74</sup> whereas the analysis of rat and human promoters showed a single TSS (data not shown). We evaluate the presence of RUNX2-binding motifs in the *Adam17* promoter using the consensus RUNX2 motif 5'-(T/A/C)G(T/A/C)GG(T/G) that was previously validated in a genomic-wide occupancy study.<sup>33</sup> The mouse *Adam17* gene promoter contains at least eight RUNX2 consensus motifs (Figure 3A) whereas the analysis of rat and human promoters showed eight and three RUNX2 motifs, respectively (data not shown). The motifs 5'-TGTGGT and 5-AGTGGT, that are perfect matches respect to consensus sequence, represent 4/8 of the total putative RUNX2 motifs observed in the mouse *Adam17* promoter. Interestingly, a variable number of a one-mismatch 5'-TGTGGG RUNX2 motifs are localized close to the TSSs in the mouse *Adam17* promoter (sites Runx2 I, II, and VI). Moreover, one site ("Runx2 I") is highly conserved in the rat and human *Adam17* promoters (data not shown). This one-mismatch motif is the second most frequently observed RUNX2 motif in genomic promoters, and a large fraction of these gene promoters (~35%) is not co-occupied by RNAPII,<sup>33</sup> consistent with the model that this sequence motif may support Runx2-mediated gene repression.

To determine the functional contribution of RUNX2 to regulation of *Adam17* promoter, we performed transient transfection assays with *Adam17* mouse promoter fragments spanning 2304 bp of 5' sequence (containing eight RUNX2 motifs) in a luciferase reporter (p*Adam17*-Luc, originally described as p*Tace*-Luc),<sup>71</sup> in pre-osteoblast MC3T3-E1 cells. Specifically, we identify promoter regions implicated in RUNX2 transcriptional regulation using a series of 5' deletion constructs of the p*Adam17*-Luc vector (Figure 3B). Deletion of nt -2304 to -903 results in an increase of *Adam17* promoter activity, suggesting the presence of repressive elements in the 5' region of the distal-promoter (Figure 3C). However, deletion of nt -903 to -121 decreases promoter activity, thus also suggesting the presence of activating elements at the proximal-promoter. Interestingly,

co-expression of *Runx2* does not significantly activate or repress *Adam17* promoter at the putative RUNX2 binding sites VIII-III localized between nt -2304 to -410, but RUNX2 significantly attenuates promoter activity of the -410 bp deletion construct (nt -410 to -121) containing the RUNX2 I and II binding elements (Figure 3C). These results indicate that there are at least two functional RUNX2 binding sites located in the -410/-121 region at the proximal *Adam17* promoter that can orchestrate the RUNX2-mediated repression of this regulatory region.

Because the C-terminal domain of RUNX2 is required for its gene repressive functions, we next analyze the contribution of this region to repress activity of the -410 bp *Adam17* gene promoter in MC3T3-E1 pre-osteoblastic cells (Figure 3D). Interestingly, only wild-type *Runx2* but not the mutant version of this transcription factor (*Runx2*- $\Delta$ 361) which lacks the C-terminal region results in significant reductions of the -410 *Adam17* promoter in osteoblastic cells, indicating that *Adam17* gene repression by RUNX2 requires the C-terminal region (Figure 3E).

### 3.4 | *Adam17* gene expression is reduced during osteoblastic differentiation

To address whether *Adam17* downregulation is biological coupled to the physiologic upregulation of RUNX2 observed during MC3T3-E1 osteoblast differentiation, we analyzed endogenous expression of *Adam17* in relation to RUNX2 expression levels. Osteogenic differentiation was monitored by ALPL activity (a cognate RUNX2-target gene) (Figure 4A). We found a significant reduction of *Adam17* mRNA levels that precedes the ADAM17 decrease in both protein levels and immune staining after day 4-8, in parallel with the early elevation in *Runx2* mRNA and RUNX2 protein levels as well as RUNX2 protein nuclear immune staining (4-8 days) (Figure 4B-F). These patterns are associated with the subsequent cessation in cell proliferation and subsequent initiation of osteoblast differentiation, as evidenced by the absence of CCND1 expression after day 12 and elevation of Alpl expression between days 4-12 (Figure 4D).

### 3.5 | Proximal promoter of the *Adam17* selectively associated with RUNX2 during osteoblastic differentiation

To determine whether RUNX2 bind to the endogenous *Adam17* gene proximal promoter during osteogenic differentiation, we performed chromatin immunoprecipitation (ChIP) analysis under in vitro culture conditions that reproduce osteoblast differentiation. We tested RUNX2 binding to sites I and II at the proximal promoter (-405/-167), as well as to others in two selected regions upstream of this region (-930/-731 and -1651/-1422) that contain sites III-V and site VII,



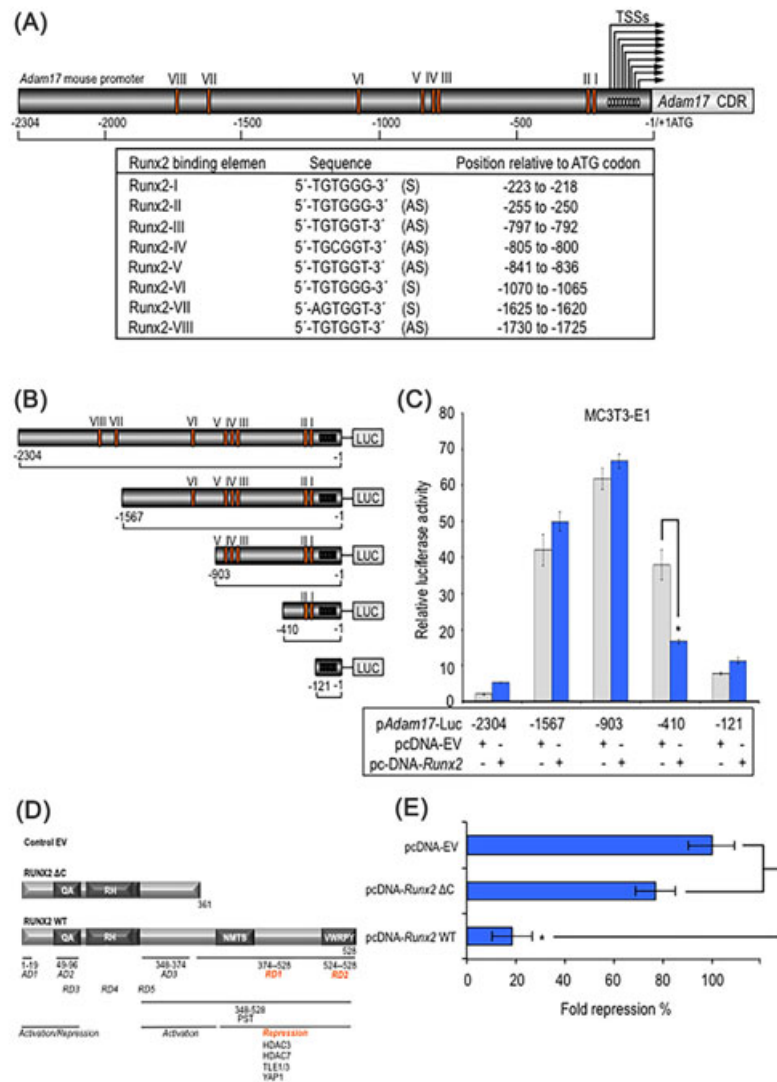


**FIGURE 3** *Adam17* promoter has a proximal region containing RUNX2 binding sites supporting transcriptional repression. *Adam17* gene promoter from mouse was analyzed for the presence of the genome-wide consensus Runx motif (5'-[A/C]CC[A/T/G]C[A/T/G]-3') previously established for us<sup>80</sup> (A). S and AS indicated sense- and antisense-stranded DNA. Arrows indicated transcription start sites (TSS) (-161 to -55, relative to ATG codon). MC3T3-E1 cells were transfected with either a luciferase reporter gene under transcriptional control of the promoter region of mouse *Adam17* (p*Adam17* 2.3-Kb) or with a series of deletion mutants spanning the mouse *Adam17* gene promoter that overexpress wild-type *Runx2* or empty vector control pcDNA 3.1 (EV) for *Runx2* expression construct (B and C). Effect of wild type *Runx2* (Runx2 WT) or deletion mutant *Runx2* 1-361 (Runx2  $\Delta$ C) expression or empty vector control pcDNA 3.1 (EV) on 0.4-Kb *Adam17* proximal promoter was also determined by a luciferase activity assay (D and E). The promoter activity was determined by a luciferase activity assay after 24 h of transient transfection and normalized by cotransfection with Renilla luciferase. All data are presented as mean  $\pm$  SEM from three independent experiments. \* $P < 0.05$ .

respectively (Figure 5A). The data provide further in vivo evidence showing that RUNX2 selectively binds to the proximal promoter of the *Adam17* gene, containing the RUNX2 I, and II binding elements in pre-osteoblast MC3T3-E1 cells (Figure 5B). ChIP analyses also revealed that RUNX2 differentially binds to the 5'-proximal promoter of *Adam17* and that occupancy of sites I-II and sites III-IV increases significantly in differentiating osteoblasts, while the distal upstream region was not enriched in the precipitated DNA samples (Figure 5C). Taken together, our findings demonstrate

that *Adam17* gene repression during osteoblastic differentiation is associated with RUNX2 binding at the *Adam17* gene promoter.

### 3.6 | *Adam17* overexpression attenuates osteoblast differentiation

To understand the biological relevance of *Adam17* gene repression in osteoblast differentiation, we overexpressed exogenous *Adam17* above normal physiological levels in

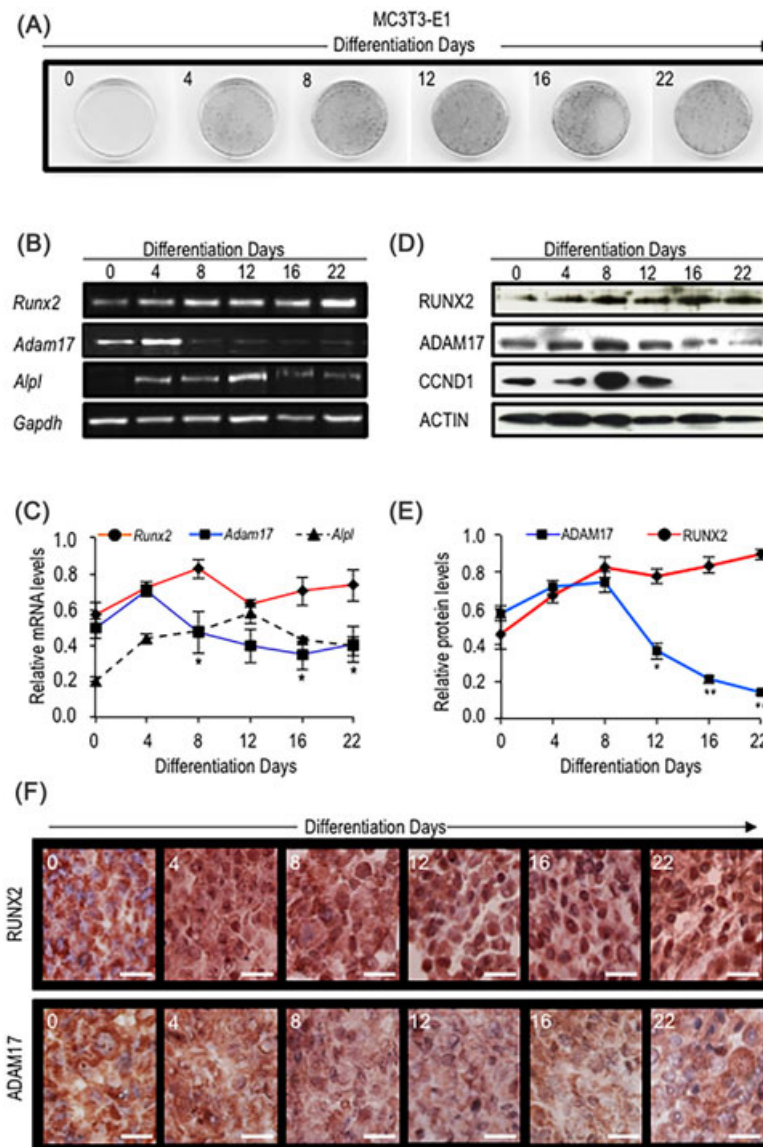


**FIGURE 4** *Adam17* expression is down-regulated during osteogenic differentiation. MC3T3-E1 cells were induced to differentiate with ascorbic acid and  $\beta$ -glycerophosphate for 28 days. Cells were fixed in paraformaldehy for histochemical detection of alkaline phosphatase at the indicated days of differentiation (day 0, 4, 8, 12, 16, 22, and 28) (A). *Adam17* and *Runx2* mRNA and protein levels as well as ADAM17 and RUNX2 cellular localization were determined by RT-PCR (B, and down graph C), Western blot (D, and down graph E) and immunostaining (F), respectively. Expression of osteoblast phenotypic genes alkaline phosphatase (*Alpl*) as well as cell cycle marker cyclin D (*Ccnd1*) were additionally examined by RT-PCR and Western blot, respectively. The data shown are representative of three experiments with similar outcomes. *Runx2* and *Adam17* mRNA (C, right graph) and protein (E, left graph) values were normalized to *Gapdh* and *Actin*, respectively. All data are presented as mean  $\pm$  SEM from three independent experiments. \* $P < 0.05$  and \*\* $P < 0.01$

differentiating MC3T3-E1 cells using a CMV-driven expression vector. *Adam17* was efficiently expressed above the normal endogenous levels in osteoblasts from day 2-6 of differentiation (Figures 6A and 6B). Moreover, *Adam17* overexpression attenuates *Runx2* expression and reduces both the expression and activity of the RUNX2-target gene *Alpl* that is normally increased during early stages of osteoblast differentiation (Figure 6C-F). Thus, our data suggest that *Adam17* expression regulates osteoblastic differentiation. Our collective findings are

consistent with a novel regulatory model in which reciprocal feedback regulation between *Runx2*-*Adam17* controls progression of osteoblast differentiation.

#### 4 | DISCUSSION

In this study, we provide evidence that expression of *Adam17*, which physiologically controls the presentation of proteins on the cell surface of osteoblasts, is a direct transcriptional target

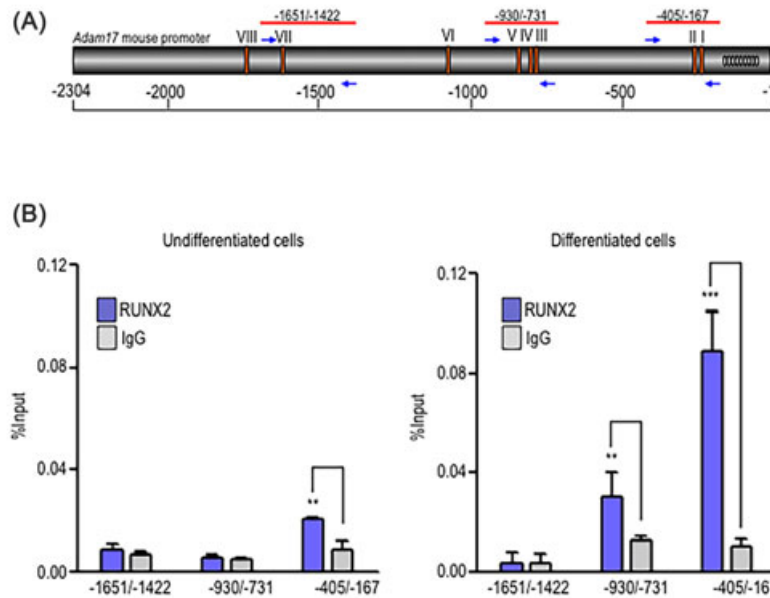


**FIGURE 5** RUNX2 binds to the *Adam17* proximal promoter region in differentiating osteoblastic cells. Diagram illustrates the location of the primers used in the ChIP experiments. Arrows indicate the direction of each primer, and the negative values indicate their position relative to ATG (A). MC3T3-E1 cells were induced to differentiate with ascorbic acid and  $\beta$ -glycerophosphate and cultured up to day 12. Undifferentiated (B) and differentiated (C) cells were cross-linked with 1% formaldehyde, and the sonicated chromatin fragments were immunoprecipitated using specific polyclonal antibodies against RUNX2 protein. The enrichment of *Adam17* promoter sequences in the precipitated chromatin fragments was quantified by qPCR using the primers described in panel A. All data are presented as mean  $\pm$  SEM from three independent experiments. \*\* $P < 0.01$  and \*\*\* $P < 0.001$

of RUNX2 during osteoblast differentiation. The role of ADAM17 in skeletal development has been previously analyzed in knockout mice in which *Adam17* was conditionally disrupted in chondrocytes and osteochondroprogenitor cells.<sup>48,63,75</sup> These studies showed that mutant mice exhibit growth retardation, reduction on femur length with impaired growth of chondroblasts, elongated hypertrophic zone, and accumulation of differentiated chondrocytes that produces a calcified matrix suggesting that ADAM17 regulates terminal differentiation of chondrocytes during endochondral ossification.<sup>48,75</sup> Interestingly, a histomorphometric analysis revealed that osteoblast-related parameters, including numbers of osteoblast, were increased in conditional *Adam17*-deficient mouse suggesting that ADAM17 may also be involved in osteoblast differentiation.<sup>63</sup>

We examined the role of RUNX2 in controlling *Adam17* expression in osteoblasts using different mouse and human cellular models included the MC3T3-E1 pre-osteoblast cell line, human osteoblasts, and the immortalized *Runx2*-null osteoprogenitor cells. Our data are consistent with microarray gene expression profiling with *Runx2* null cells expressing wild-type and mutant RUNX2 proteins, which revealed changes in the expression of several ADAM and ADAMTS members.<sup>76</sup> Moreover, examination of ChIP-microarray data sets for RUNX2 target genes in human osteoblastic cells<sup>33</sup> revealed additional genomic promoter interactions for RUNX2 on other

promoters of ADAM and ADAMTS genes (data not shown). Thus, several members of both gene families could be potential downstream target genes of RUNX2, and our data clearly show that *Adam17* is a prominent member controlled by RUNX2.

RUNX2 is a bifunctional transcription factor that may interact with a broad spectrum of co-activators and co-repressor, thus supporting activation, or repression of RUNX2 target genes. Several repression domains (RD) have been characterized in different regions of RUNX2 protein, which define binding of specific co-repressors. Specifically, the RUNX2 C-terminal region exhibits at least two different repression domains capable of interacting with several proteins involved in gene repression like histone deacetylases (HDACs).<sup>77–79</sup> The RUNX2 C-terminal region may support transcriptional repression of *Adam17* gene through interactions with HDACs or other chromatin related co-repressors. Interestingly, previous reports showed that RUNX2 can positively regulate expression of *Adamts4* and *Adamts5* in chondrocytes,<sup>58–60,62</sup> perhaps suggesting that *Runx2* may have a bifunctional role during osteogenesis.

ADAM17 was initially characterized as an enzyme anchored to the plasma membrane which is involved in proteolytic processing and the release of TNF- $\alpha$  to the extracellular milieu. Interestingly, TNF- $\alpha$  (TNF) inhibits extracellular matrix maturation and mineralization in osteoblasts by decreasing production of type I collagen, a key

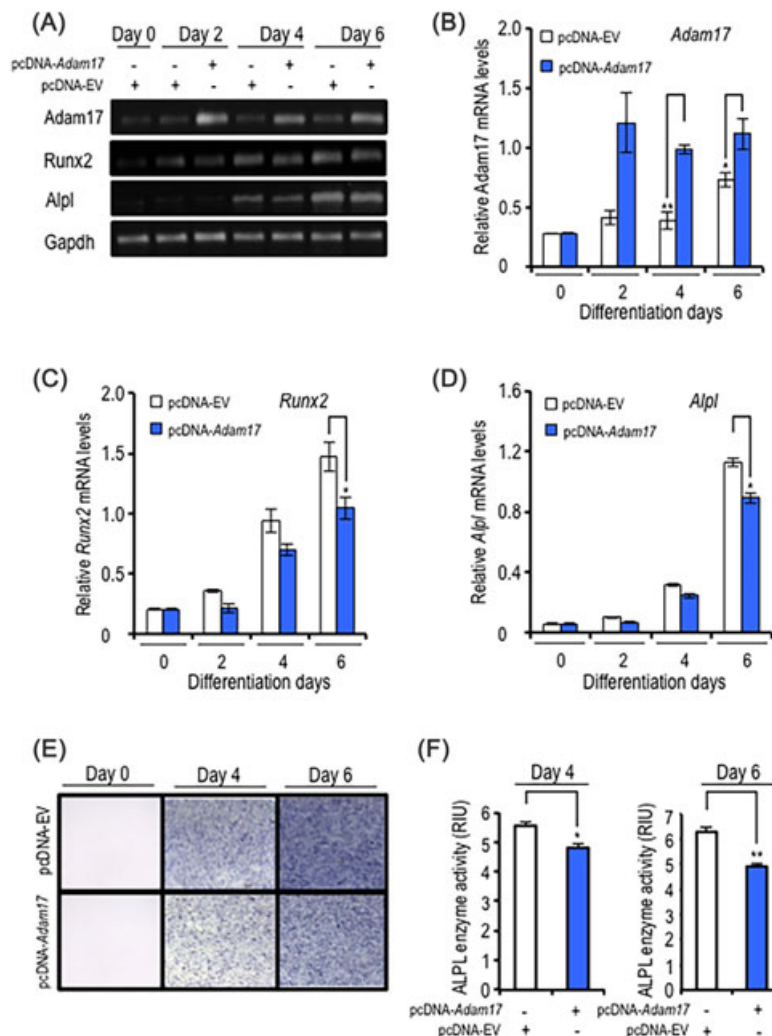


**FIGURE 6** *Adam17* expression affects osteoblastic differentiation. MC3T3-E1 cells were transfected with a construct expressing *Adam17* or control empty vector (EV). Cells were induced to differentiate at 24 h after transfection with ascorbic acid and  $\beta$ -glycerophosphate for 6 days. Expression of *Adam17*, *Runx2*, and alkaline phosphatase (*Alpl*) were examined by RT-PCR at day 0, 2, 4, and 6 of differentiation (A). *Adam17* (B), *Runx2* (C) and *Alpl* mRNA (D) values normalized to *Gapdh*. Additionally, cells were fixed in paraformaldehy for histochemical detection of alkaline phosphatase at the indicated days of differentiation (day 0, 4, and 6) (E). Histochemical staining of ALP activity was quantified using Image J processing software and values were expressed in relative intensity units (RIU) (F). All data are presented as mean  $\pm$  SEM from three independent experiments. \* $P < 0.05$  and \*\* $P < 0.01$

component of a mature skeletal matrix, and by evoking an attenuated response to vitamin D associated with reduced ALPL activity, and osteocalcin/BGLAP release.<sup>80,81</sup> In addition, TNF- $\alpha$  also induces a reduction of the IGF-1 expression, a growth factor that is known to promote osteoblast differentiation.<sup>64</sup> Other studies have shown that TNF- $\alpha$  downregulated expression of BMPR and attenuated BMP-2-mediate *Alpl* and *Oc/Bglap* expression in human bone cells.<sup>82</sup> Moreover, TNF- $\alpha$  inhibits osteoblast differentiation through the inhibition of mineralized nodule formation and inhibition of *Runx2* and *Osx/Sp7* expression, both master genes of the osteoblast differentiation, and skeletal-specific genes (eg *Alpl*, *Bsp/Ibsp*, *Oc/Bglap*).<sup>83–86</sup> Hence, our results could be envisioned as part of a RUNX2-ADAM17-TNF

axis. In this model, the osteogenic activation of RUNX2 stimulates osteoblast differentiation by preventing the ADAM17-mediated release of TNF which otherwise suppresses osteoblast maturation. Negative regulation of RUNX2 by ADAM17 may ensure that this axis only works when RUNX2 levels have reached a critical threshold.

On the other hand, ADAM17 protein also releases a soluble form of the membrane-anchored DLK1 protein (named fetal antigen 1, FA1) in mesenchymal precursors<sup>87–89</sup> and pre-osteoblastic cells.<sup>90</sup> Pre-osteoblastic cells treated with soluble DLK1 or overexpressing *Dlk1* exhibit elevated *Sox9* expression that prevents osteoblast differentiation and *Runx2* expression.<sup>90</sup> Hence, it is reasonable to propose that the results observed following *Adam17* overexpression in osteoblastic



10. Li Y, Ge C, Franceschi RT. MAP kinase-dependent RUNX2 phosphorylation is necessary for epigenetic modification of chromatin during osteoblast differentiation. *J Cell Physiol.* 2016; 232:2427–2435.
11. Liu JC, Lengner CJ, Gaur T, et al. Runx2 protein expression utilizes the Runx2 P1 promoter to establish osteoprogenitor cell number for normal bone formation. *J Biol Chem.* 2011;286:30057–30070.
12. Yoshida CA, Komori H, Maruyama Z, et al. SP7 inhibits osteoblast differentiation at a late stage in mice. *PLoS ONE.* 2012;7:e32364.
13. Okura H, Sato S, Kishikawa S, et al. Runx2-I isoform contributes to fetal bone formation even in the absence of specific N-terminal amino acids. *PLoS ONE.* 2014;9:e108294.
14. Lim KE, Park NR, Che X, et al. Core binding factor  $\beta$  of osteoblasts maintains cortical bone mass via stabilization of Runx2 in mice. *J Bone Miner Res.* 2015;30:715–722.
15. Qin X, Jiang Q, Matsuo Y, et al. Cbfb regulates bone development by stabilizing Runx family proteins. *J Bone Miner Res.* 2015;30:706–714.
16. Takarada T, Nakazato R, Tsuchikane A, et al. Genetic analysis of Runx2 function during intramembranous ossification. *Development.* 2016;143:211–218.
17. Hovhannisyan H, Zhang Y, Hassan MQ, et al. Genomic occupancy of HLH, AP1 and Runx2 motifs within a nuclease sensitive site of the Runx2 gene. *J Cell Physiol.* 2013;228:313–321.
18. Barutcu AR, Tai PW, Wu H, et al. The bone-specific Runx2-P1 promoter displays conserved three-dimensional chromatin structure with the syntenic Supt3h promoter. *Nucleic Acids Res.* 2014;42:10360–10372.
19. Kawane T, Komori H, Liu W, et al. Dlx5 and mef2 regulate a novel runx2 enhancer for osteoblast-specific expression. *J Bone Miner Res.* 2014;29:1960–1969.
20. Tai PW, Wu H, Gordon JA, et al. Epigenetic landscape during osteoblastogenesis defines a differentiation-dependent Runx2 promoter region. *Gene.* 2014;550:1–9.
21. Rojas A, Aguilar R, Henriquez B, et al. Epigenetic control of the bone-master runx2 gene during osteoblast-lineage commitment by the histone demethylase JARID1B/KDM5B. *J Biol Chem.* 2015;290:28329–28342.
22. Aguilar R, Bustos FJ, Saez M, et al. Polycomb PRC2 complex mediates epigenetic silencing of a critical osteogenic master regulator in the hippocampus. *Biochim Biophys Acta.* 2016;1859:1043–1055.
23. Kapinas K, Kessler C, Ricks T, Gronowicz G, Delany AM. MiR-29 modulates Wnt signaling in human osteoblasts through a positive feedback loop. *J Biol Chem.* 2010;285:25221–25231.
24. Zhang Y, Xie RL, Croce CM, et al. A program of microRNAs controls osteogenic lineage progression by targeting transcription factor Runx2. *Proc Natl Acad Sci U S A.* 2011;108:9863–9868.
25. Lian JB, Stein GS, van Wijnen AJ, et al. MicroRNA control of bone formation and homeostasis. *Nat Rev Endocrinol.* 2012;8:212–227.
26. Zhang Y, Xie RL, Gordon J, et al. Control of mesenchymal lineage progression by microRNAs targeting skeletal gene regulators Trps1 and Runx2. *J Biol Chem.* 2012;287:21926–21935.
27. Smith SS, Dole NS, Franceschetti T, Hrdlicka HC, Delany AM. MicroRNA-433 dampens glucocorticoid receptor signaling, impacting circadian rhythm and osteoblastic gene expression. *J Biol Chem.* 2016;291:21717–21728.
28. Varela N, Aranguiz A, Lizama C, et al. Mitotic inheritance of mRNA facilitates translational activation of the osteogenic-Lineage commitment factor runx2 in progeny of osteoblastic cells. *J Cell Physiol.* 2016;231:1001–1014.
29. Teplyuk NM, Haupt LM, Ling L, et al. The osteogenic transcription factor Runx2 regulates components of the fibroblast growth factor/proteoglycan signaling axis in osteoblasts. *J Cell Biochem.* 2009; 107:144–154.
30. Teplyuk NM, Zhang Y, Lou Y, et al. The osteogenic transcription factor runx2 controls genes involved in sterol/steroid metabolism, including CYP11A1 in osteoblasts. *Mol Endocrinol.* 2009;23:849–861.
31. Hawse JR, Cicek M, Grygo SB, et al. TIEG1/KLF10 modulates Runx2 expression and activity in osteoblasts. *PLoS ONE.* 2011;6: e19429.
32. Purcell DJ, Khalid O, Ou CY, et al. Recruitment of coregulator G9a by Runx2 for selective enhancement or suppression of transcription. *J Cell Biochem.* 2012;113:2406–2414.
33. van der Deen M, Akech J, Lapointe D, et al. Genomic promoter occupancy of runt-related transcription factor RUNX2 in Osteosarcoma cells identifies genes involved in cell adhesion and motility. *J Biol Chem.* 2012;287:4503–4517.
34. McGee-Lawrence ME, Li X, Bledsoe KL, et al. Runx2 protein represses Axin2 expression in osteoblasts and is required for craniosynostosis in Axin2-deficient mice. *J Biol Chem.* 2013;288:5291–5302.
35. McGee-Lawrence ME, Bradley EW, Dudakovic A, et al. Histone deacetylase 3 is required for maintenance of bone mass during aging. *Bone.* 2013;52:296–307.
36. Yang D, Okamura H, Nakashima Y, Haneji T. Histone demethylase Jmjd3 regulates osteoblast differentiation via transcription factors Runx2 and osterix. *J Biol Chem.* 2013;288:33530–33541.
37. Meyer MB, Benkusky NA, Pike JW. The RUNX2 cistrome in osteoblasts: characterization, down-regulation following differentiation, and relationship to gene expression. *J Biol Chem.* 2014;289: 16016–16031.
38. Wu H, Whitfield TW, Gordon JA, et al. Genomic occupancy of Runx2 with global expression profiling identifies a novel dimension to control of osteoblastogenesis. *Genome Biol.* 2014;15:R52.
39. Inoue D, Reid M, Lum L, et al. Cloning and initial characterization of mouse meltrin beta and analysis of the expression of four metalloprotease-disintegrins in bone cells. *J Biol Chem.* 1998;273: 4180–4187.
40. Dallas DJ, Genever PG, Patton AJ, Millichip MI, McKie N, Skerry TM. Localization of ADAM10 and Notch receptors in bone. *Bone.* 1999;25:9–15.
41. Mohan S, Thompson GR, Amaar YG, Hathaway G, Tschesche H, Baylink DJ. ADAM-9 is an insulin-like growth factor binding protein-5 protease produced and secreted by human osteoblasts. *Biochemistry.* 2002;41:15394–15403.
42. Pan B, Farrugia AN, To LB, et al. The nitrogen-containing bisphosphonate, zoledronic acid, influences RANKL expression in human osteoblast-like cells by activating TNF-alpha converting enzyme (TACE). *J Bone Miner Res.* 2004;19:147–154.
43. Franchimont N, Lambert C, Huynen P, et al. Interleukin-6 receptor shedding is enhanced by interleukin-1beta and tumor necrosis factor alpha and is partially mediated by tumor necrosis factor alpha-converting enzyme in osteoblast-like cells. *Arthritis Rheum.* 2005;52:84–93.
44. Chan KM, Wong HL, Jin G, et al. MT1-MMP inactivates ADAM9 to regulate FGFR2 signaling and calvarial osteogenesis. *Dev Cell.* 2012;22:1176–1190.
45. Tan Y, Fu R, Liu J, et al. ADAM10 is essential for cranial neural crest-derived maxillofacial bone development. *Biochem Biophys Res Commun.* 2016;475:308–314.

46. Hikita A, Yana I, Wakeyama H, et al. Negative regulation of osteoclastogenesis by ectodomain shedding of receptor activator of NF-kappaB ligand. *J Biol Chem*. 2006;281:36846–36855.
47. Karadag A, Zhou M, Croucher PI. ADAM-9 (MDC-9/meltrin-gamma), a member of the a disintegrin and metalloproteinase family, regulates myeloma-cell-induced interleukin-6 production in osteoblasts by direct interaction with the alpha(v)beta5 integrin. *Blood*. 2006;107:3271–3278.
48. Hall KC, Hill D, Otero M, et al. ADAM17 controls endochondral ossification by regulating terminal differentiation of chondrocytes. *Mol Cell Biol*. 2013;33:3077–3090.
49. Zhou J, Fujiwara T, Ye S, Li X, Zhao H. Downregulation of Notch modulators, tetraspanin 5 and 10, inhibits osteoclastogenesis in vitro. *Calcif Tissue Int*. 2014;95:209–217.
50. Harris HA, Murrills RJ, Komm BS. Expression of meltrin-alpha mRNA is not restricted to fusagenic cells. *J Cell Biochem*. 1997; 67:136–142.
51. Kurisaki T, Masuda A, Osumi N, Nabeshima Y, Fujisawa-Sehara A. Spatially- and temporally-restricted expression of meltrin alpha (ADAM12) and beta (ADAM19) in mouse embryo. *Mech Dev*. 1998;73:211–215.
52. Miles RR, Sluka JP, Halladay DL, et al. ADAMTS-1: A cellular disintegrin and metalloprotease with thrombospondin motifs is a target for parathyroid hormone in bone. *Endocrinology*. 2000; 141:4533–4542.
53. Verrier S, Hogan A, McKie N, Horton M. ADAM gene expression and regulation during human osteoclast formation. *Bone*. 2004;35:34–46.
54. Lind T, McKie N, Wendel M, Racey SN, Birch MA. The hyalactan degrading ADAMTS-1 enzyme is expressed by osteoblasts and up-regulated at regions of new bone formation. *Bone*. 2005;36: 408–417.
55. Nakamura M, Sone S, Takahashi I, Mizoguchi I, Echigo S, Sasano Y. Expression of versican and ADAMTS1, 4, and 5 during bone development in the rat mandible and hind limb. *J Histochem Cytochem*. 2005;53:1553–1562.
56. Rehn AP, Birch MA, Karlström E, Wendel M, Lind T. ADAMTS-1 increases the three-dimensional growth of osteoblasts through type I collagen processing. *Bone*. 2007;41:231–238.
57. Govoni KE, Ameer YG, Kramer A, Winter E, Baylink DJ, Mohan S. Regulation of insulin-like growth factor binding protein-5, four and a half lim-2, and a disintegrin and metalloprotease-9 expression in osteoblasts. *Growth Horm IGF Res*. 2006;16:49–56.
58. Thirunavukkarasu K, Pei Y, Moore TL, et al. Regulation of the human ADAMTS-4 promoter by transcription factors and cytokines. *Biochem Biophys Res Commun*. 2006;345:197–204.
59. Thirunavukkarasu K, Pei Y, Wei T. Characterization of the human ADAMTS-5 (aggrecanase-2) gene promoter. *Mol Biol Rep*. 2007; 34:225–231.
60. Lin AC, Seeto BL, Bartoszko JM, et al. Modulating hedgehog signaling can attenuate the severity of osteoarthritis. *Nat Med*. 2009;15:1421–1425.
61. Kadri A, Funck-Brentano T, Lin H, et al. Inhibition of bone resorption blunts osteoarthritis in mice with high bone remodelling. *Ann Rheum Dis*. 2010;69:1533–1538.
62. Tetsunaga T, Nishida K, Furumatsu T, et al. Regulation of mechanical stress-induced MMP-13 and ADAMTS-5 expression by RUNX-2 transcriptional factor in SW1353 chondrocyte-like cells. *Osteoarthritis Cartilage*. 2011;19:222–232.
63. Horiuchi K, Kimura T, Miyamoto T, et al. Conditional inactivation of TACE by a Sox9 promoter leads to osteoporosis and increased granulopoiesis via dysregulation of IL-17 and G-CSF. *J Immunol*. 2009;182:2093–20101.
64. Gilbert L, He X, Farmer P, et al. Inhibition of osteoblast differentiation by tumor necrosis factor-alpha. *Endocrinology*. 2000;141:3956–3964.
65. Bae JS, Gutierrez S, Narla R, et al. Reconstitution of Runx2/Cbfa1-null cells identifies a requirement for BMP2 signaling through a Runx2 functional domain during osteoblast differentiation. *J Cell Biochem*. 2007;100:434–449.
66. Lewallen EA, Jones DL, Dudakovic A, et al. Osteogenic potential of human adipose-tissue-derived mesenchymal stromal cells cultured on 3D-printed porous structured titanium. *Gene*. 2016; 581:95–106.
67. Pratap J, Galindo M, Zaidi SK, et al. Cell growth regulatory role of Runx2 during proliferative expansion of preosteoblasts. *Cancer Res*. 2003;63:5357–5362.
68. Galindo M, Pratap J, Young DW, et al. The bone-specific expression of Runx2 oscillates during the cell cycle to support a G1-related antiproliferative function in osteoblasts. *J Biol Chem*. 2005;280:20274–20285.
69. Galindo M, Kahler RA, Teplyuk NM, et al. Cell cycle related modulations in Runx2 protein levels are independent of lymphocyte enhancer-binding factor 1 (Lef1) in proliferating osteoblasts. *J Mol Histol*. 2007;38:501–506.
70. Dudakovic A, Camilleri E, Riester SM, et al. High-resolution molecular validation of self-renewal and spontaneous differentiation in clinical-grade adipose-tissue derived human mesenchymal stem cells. *J Cell Biochem*. 2014;115:1816–1828.
71. Charbonneau M, Harper K, Grondin F, et al. Hypoxia-inducible factor mediates hypoxic and tumor necrosis factor alpha-induced increases in tumor necrosis factor-alpha converting enzyme/ADAM17 expression by synovial cells. *J Biol Chem*. 2007;282: 33714–33724.
72. van der Deen M, Hassan MQ, Pratap J, et al. Chromatin immunoprecipitation assays: application of ChIP-on-chip for defining dynamic transcriptional mechanisms in bone cells. *Methods Mol Biol*. 2008;455:165–176.
73. Balint E, Lapointe D, Drissi H, et al. Phenotype discovery by gene expression profiling: mapping of biological processes linked to BMP-2-mediated osteoblast differentiation. *J Cell Biochem*. 2003; 89:401–426.
74. Mizui Y, Yamazaki K, Sagane K, Tanaka I. CDNA cloning of mouse tumor necrosis factor-alpha converting enzyme (TACE) and partial analysis of its promoter. *Gene*. 1999;233:67–74.
75. Saito K, Horiuchi K, Kimura T, et al. Conditional inactivation of TNF $\alpha$ -Converting enzyme in chondrocytes results in an elongated growth plate and shorter long bones. *PLoS ONE*. 2013;8:e54853.
76. Teplyuk NM, Galindo M, Teplyuk VI, et al. Runx2 regulates G protein-coupled signaling pathways to control growth of osteoblast progenitors. *J Biol Chem*. 2008;283:27585–27597.
77. Bradley EW, Carpio LR, van Wijnen AJ, McGee-Lawrence ME, Westendorf JJ. Histone deacetylases in bone development and skeletal disorders. *Physiol Rev*. 2015;95:1359–13581.
78. Westendorf JJ. Transcriptional co-repressors of Runx2. *J Cell Biochem*. 2006;98:54–64.
79. Ziros PG, Basdra EK, Papavassiliou AG. Runx2: of bone and stretch. *Int J Biochem Cell Biol*. 2008;40:1659–1663.

80. Smith DD, Gowen M, Mundy GR. Effects of interferon-gamma and other cytokines on collagen synthesis in fetal rat bone cultures. *Endocrinology*. 1987;120:2494–2499.
81. Gowen M, MacDonald BR, Russell RG. Actions of recombinant human gamma-interferon and tumor necrosis factor alpha on the proliferation and osteoblastic characteristics of human trabecular bone cells in vitro. *Arthritis Rheum*. 1988;31:1500–1507.
82. Singhatanadgit W, Salih V, Olsen I. Bone morphogenetic protein receptors and bone morphogenetic protein signaling are controlled by tumor necrosis factor-alpha in human bone cells. *Int J Biochem Cell Biol*. 2006;38:1794–1807.
83. Gilbert L, He X, Farmer P, et al. Expression of the osteoblast differentiation factor RUNX2 (Cbfa1/AML3/Pebp2alphaA) is inhibited by tumor necrosis factor-alpha. *J Biol Chem*. 2002;277:2695–26701.
84. Gilbert LC, Rubin J, Nanes MS. The p55 TNF receptor mediates TNF inhibition of osteoblast differentiation independently of apoptosis. *Am J Physiol Endocrinol Metab*. 2005;288:1011–1018.
85. Lu X, Gilbert L, He X, Rubin J, Nanes MS. Transcriptional regulation of the osterix (Osx, Sp7) promoter by tumor necrosis factor identifies disparate effects of mitogen-activated protein kinase and NF kappa B pathways. *J Biol Chem*. 2006;281:6297–62306.
86. Gilbert LC, Chen H, Lu X, Nanes MS. Chronic low dose tumor necrosis factor- $\alpha$  (TNF) suppresses early bone accrual in young mice by inhibiting osteoblasts without affecting osteoclasts. *Bone*. 2013;56:174–183.
87. Abdallah BM, Jensen CH, Gutierrez G, Leslie RG, Jensen TG, Kassem M. Regulation of human skeletal stem cells differentiation by Dlk1/Pref-1. *J Bone Miner Res*. 2004;19:841–852.
88. Taipaleenmäki H, Harkness L, Chen L, et al. The crosstalk between transforming growth factor- $\beta$ 1 and delta like-1 mediates early chondrogenesis during embryonic endochondral ossification. *Stem Cells*. 2012;30:304–313.
89. Abdallah BM, Jafari A, Zaher W, Qiu W, Kassem M. Skeletal (stromal) stem cells: an update on intracellular signaling pathways controlling osteoblast differentiation. *Bone*. 2015;70:28–36.
90. Wang Y, Sul HS. Pref-1 regulates mesenchymal cell commitment and differentiation through Sox9. *Cell Metab*. 2009;9:287–302.
91. Hilton MJ, Tu X, Wu X, et al. Notch signaling maintains bone marrow mesenchymal progenitors by suppressing osteoblast differentiation. *Nat Med*. 2008;14:306–314.
92. Engin F, Yao Z, Yang T, et al. Dimorphic effects of Notch signaling in bone homeostasis. *Nat Med* 2008;14:299–305.
93. Nakamura T, Toita H, Yoshimoto A, et al. Potential involvement of Twist2 and Erk in the regulation of osteoblastogenesis by HB-EGF-EGFR signaling. *Cell Struct Funct*. 2010;35:53–61.
94. Zanotti S, Canalis E. Notch and the skeleton. *Mol Cell Biol*. 2010;30:886–896.
95. Zunke F, Rose-John S. The shedding protease ADAM17: Physiology and pathophysiology. *Biochim Biophys Acta Molecular Cell Research*. 2017;1864:2059–2070.

**How to cite this article:** Araya HF, Sepulveda H, Lizama CO, et al. Expression of the ectodomain-releasing protease ADAM17 is directly regulated by the osteosarcoma and bone-related transcription factor RUNX2. *J Cell Biochem*. 2018;119:8204–8219. <https://doi.org/10.1002/jcb.26832>